Ultrahigh-plex to High-throughput Spatial Phenotyping: An Integrated Pathway from Discovery to Translational and Clinical Studies

Matthew McFarlane[1], Lorcan Sherry[1], Aditya Pratapa[2], Ning Ma[2], Niyati Jhaveri[2]

[1]OracleBio Ltd, Glasgow, Scotland, UK [2]Akoya Biosciences, Inc, Marlborough, Massachusetts, USA

Email contact: matthew.mcfarlane@oraclebio.com

Background & Methods

The pathway from discovery to clinical adoption of predictive spatial biomarkers (spatial signatures) for immunotherapy response requires a solution that effectively bridges ultrahigh-plex discovery experiments with targeted high-throughput translational and clinical studies. A critical step toward ensuring the successful transition is the harmonizing of technologies for staining, imaging, and data analysis. The aim of this study is to demonstrate how the integration of spatial multiplexed imaging technologies and associated data analysis methods provides an effective workflow for the spatial phenotyping of the tumor microenvironment (TME) across the discovery to clinical continuum.

Here we profiled an array of human formalin-fixed, paraffin-embedded (FFPE) cancer tissues using ultrahigh-plex PhenoCode Discovery panels (PDP) comprising of cell lineage, structural, immune activation, and checkpoint markers on the PhenoCycler®-Fusion (PCF) spatial biology platform (Figure 1). This was followed by running PhenoCode™ Signature panels (PSP) targeted to key biomarkers of immune contexture, macrophage polarization, and T cell activation status identified from the discovery studies in high-throughput experiments using the PhenoImager® HT platform. Image analysis was performed using Visiopharm's deep learning algorithms on multiplexed images to segment specific tissue regions of interest (ROI) and to perform accurate cell detection and classification of different cell phenotypes (Figure 2-5). Spatial interactions among the cell-types were also explored using spatial neighborhood analysis.

Figure 1: Ultrahigh-plex PhenoCode Discovery panels and PhenoCode™ Signature panels during discovery to clinical adoption

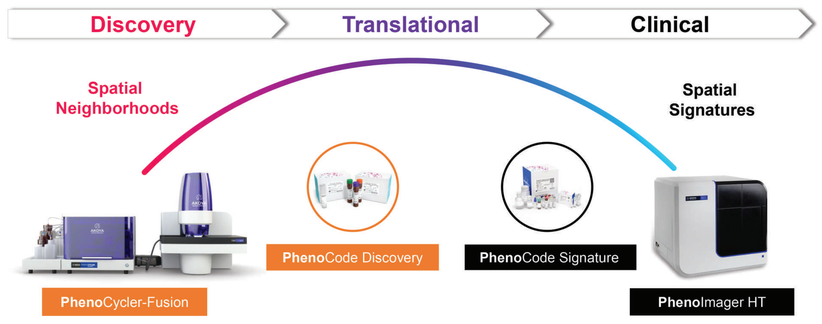

Immune Cell Profiling Core	CD8*, CD44, HLA-DR, CD4, CD45, Ki67, CD45RO, CD14, CD20, HLA-A, CD68*, CD3e, CD11b, CD163*
Immune Activation and Proliferation Module	PD-1*, PD-L1*, IDO1, PCNA, HLA-E
Advanced Lymphocyte Profiling Module	FOXP3, CD79a, CD38, CD39
Structural Module	E-Cadherin/PanCK*, Vimentin, Collagen IV, CD31, SMA, CD34, b-Catenin-1, Beta-actin, Caveolin

*Same markers are in PhenoCode Signature M1/M2 Polarization Human Protein Panel

Figure 2: Imaging of Human Breast Cancer (A) and Lymphoma (H) using the PhenoCode Signature M1/M2 Polarization Human Protein Panel and higher magnification images (B-G, I-N)

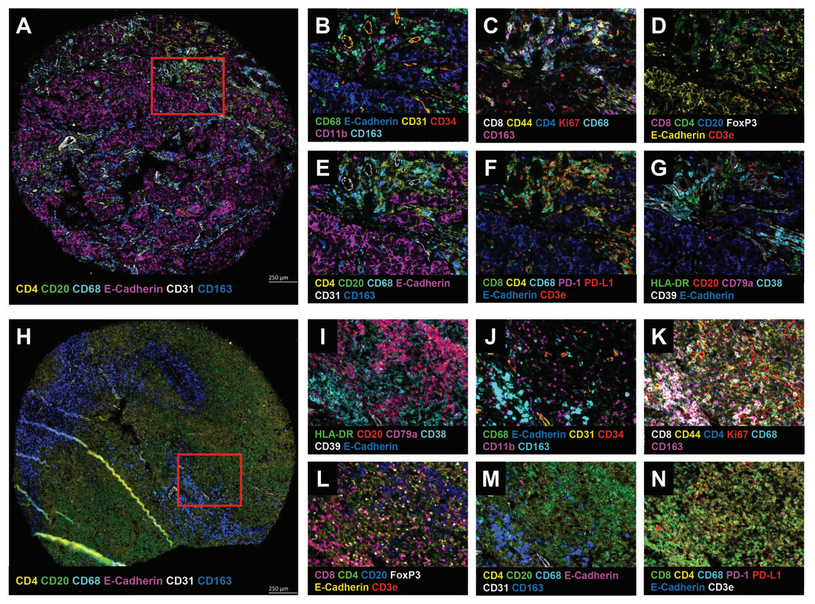

Figure 3: Image Analysis workflow

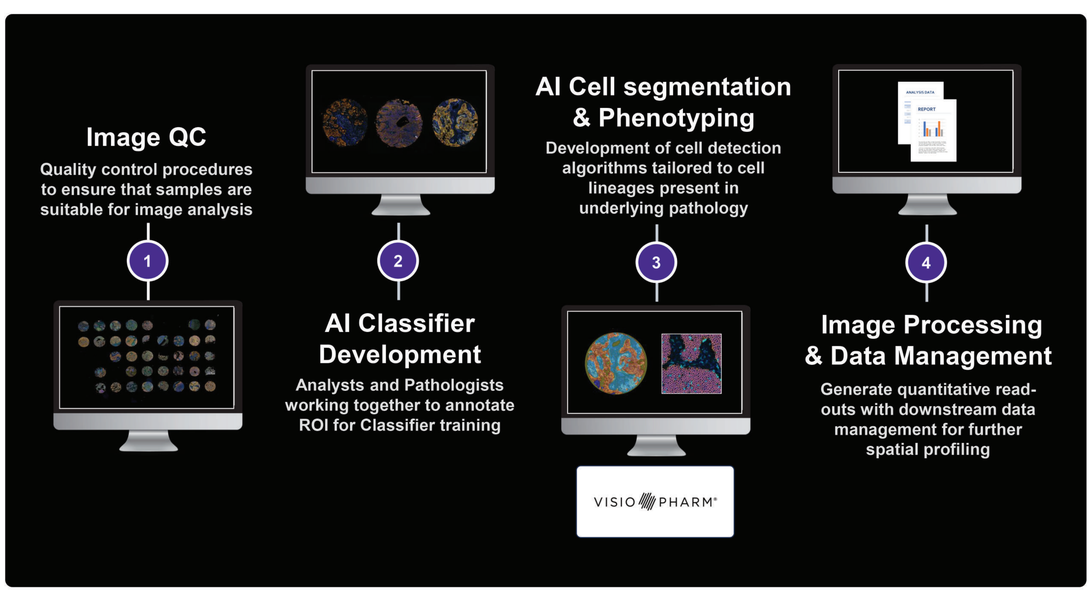

Figure 4: AI-based ROI Classification in Breast Cancer Core

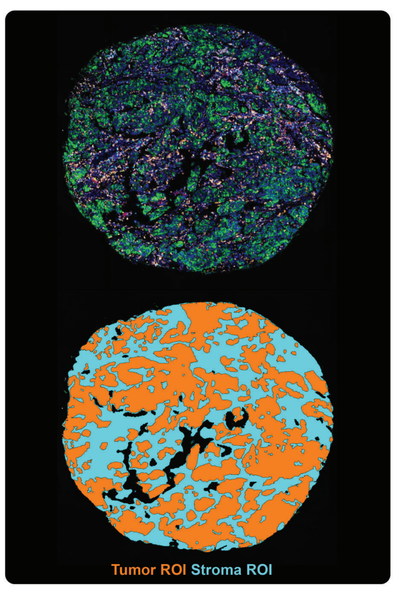

Figure 5: Example Cell Segmentation using AI Deep Learning for Immune cells (A-D) and Macrophages (E-H) in Breast Cancer Core

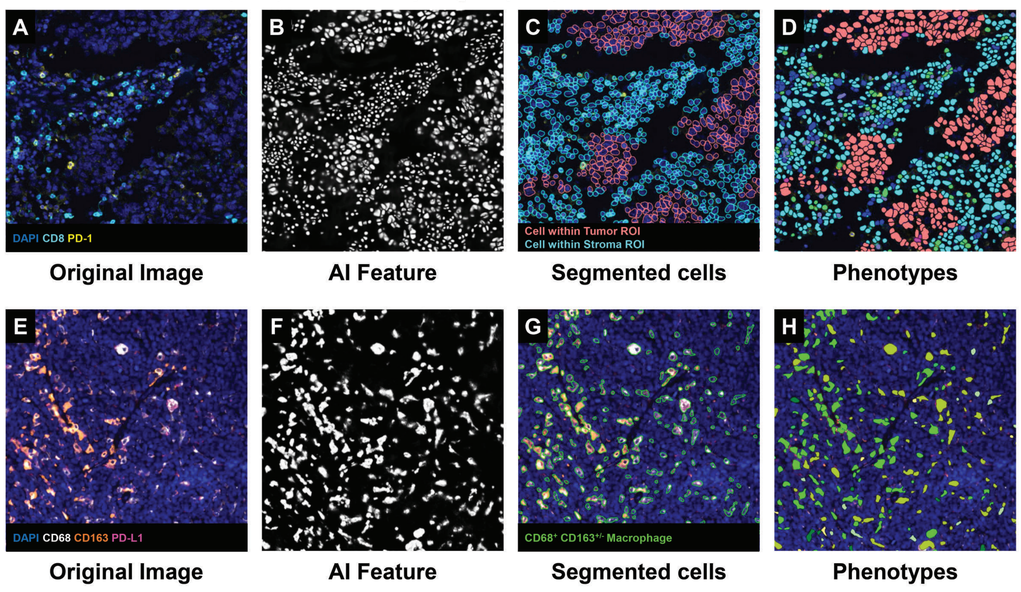

Results

Figure 6: Correlation of total CD8⁺ and total Macrophage cells detected across cores stained with 6-plex and 32-plex assays

Data evaluation from the PhenoCode Discovery and PhenoCode Signature panels focussed on Tumor-associated macrophage (TAMs) and cytotoxic Immune cell phenotypes. Good correlation was observed across both assay-stained TMAs for total CD8⁺ immune cells (R^2 = 0.89) and CD68⁺ and/or CD163⁺ macrophages (R^2 = 0.91) in respective cores. Several cell phenotypes were identified with both assays covering CD68/CD163/PD-L1 and CD8/PD-1 markers.

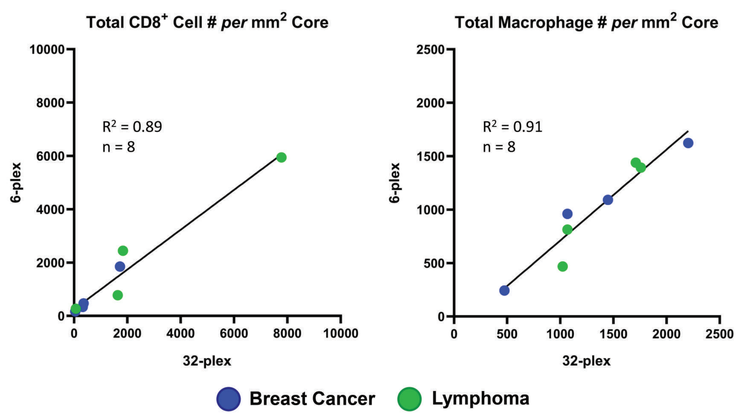

Figure 7: Immune phenotypes as % of total cells per ROI across each core stained with 6-plex assay

Immune cell phenotypes (as a % of total cells per ROI) varied across Breast Cancer (BC) cores, with numbers tending to be higher in Stroma compared to tumor and the CD8+PD-1- phenotype being more predominant than the CD8⁺PD-1⁺ phenotype across both ROI. As expected, Lymphoma cores generally contained more immune cells than BC, with some cores having a high overall % of CD8⁺PD-1⁺ cells.

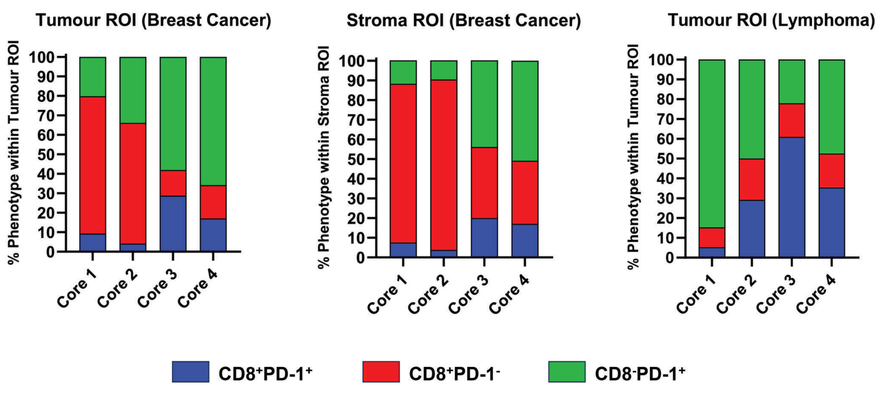

Figure 8: Macrophage phenotypes as % of total Macrophage cells per ROI across each core stained with 6-plex assay

Macrophage cells presented in various shapes and sizes, from medium to large spindle shaped cells to smaller, rounder, cells. Macrophage CD68⁺CD163⁻ and CD68⁺CD163⁺ sub-phenotypes were observed in similar number across BC and Lymphoma cores with a smaller proportion of both subtypes showing positivity for PD-L1.

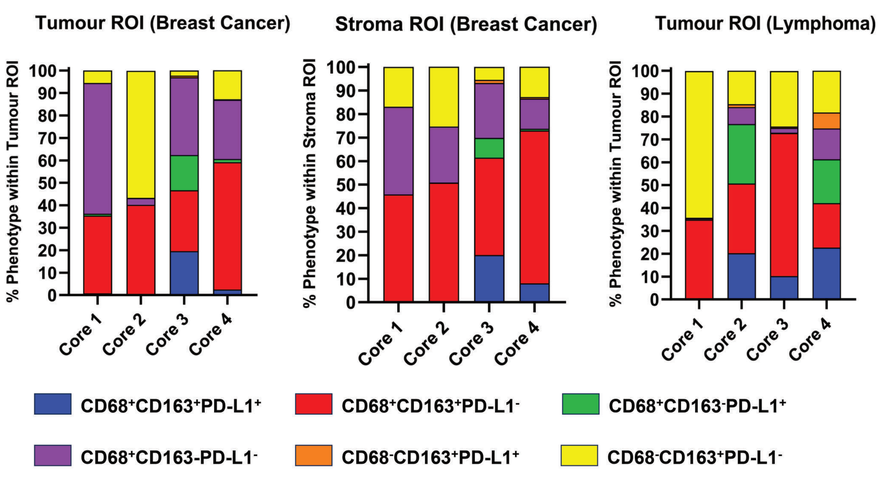

* For Research Use Only. Not for use in diagnostic procedures.

Figure 9: Example spatial analysis data from (A) Breast cancer core A04 and Lymphoma core (B02)

Example spatial analysis was performed on a representative core from each cancer type using the cell object data (x, y coordinates) generated from the Visiopharm software. Exported data was processed using a proprietary Python script and demonstrated that across both cancer types, there was closer proximity of CD8⁺ cells to macrophages of the M2 subtype compared to the M1 subtype. Also, a good correlation was observed across some readouts upon comparison of the spatial data calculated across the 32- and 6-plex TMAs, demonstrating transferability of spatial signatures from discovery to translation studies (R^2 = 0.79).

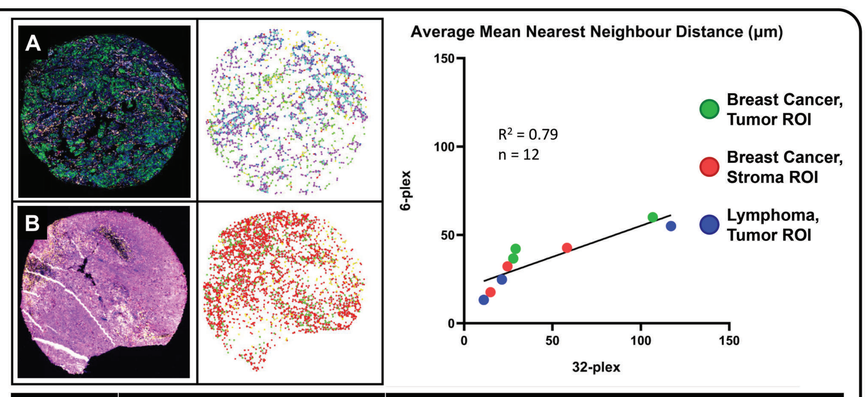

Tissue	Spatial Interactions	Average Mean Nearest Neighbour Distance (µm)			
		32-plex Tumour	32-plex Stroma	6-plex Tumour	6-plex Stroma
Breast Core (Core A04)	CD8⁺ cells to CD68⁺CD163⁻ cells	106.79	58.21	59.96	42.69
	CD8⁺ cells to CD68⁺/⁻CD163⁺	27.80	15.00	36.61	17.61
	CD68⁺CD163⁻ to CD68⁺/⁻CD163⁺	29.20	24.60	42.15	32.16
Lymphoma (Core B02)	CD8⁺ cells to CD68⁺CD163⁻ cells	117.12	NA	54.95	NA
	CD8⁺ cells to CD68⁺/⁻CD163⁺	11.13	NA	13.26	NA
	CD68⁺CD163⁻ to CD68⁺/⁻CD163⁺	21.41	NA	24.75	NA

Conclusions

We have profiled two cancer types and quantified immune cell distributions, phenotypes, and their spatial interactions. We have also utilised AI Deep Learning approaches within the analysis workflow to aid more accurate cell segmentation and management of marker stain variations across individual tissue cores. In conclusion, the combination of ultrahigh-plex discovery panels, targeted high-throughput signature panels and deep learning quantitative image analysis allows for deeper characterization of complex cellular interactions in the tumor microenvironment and shortens the development path to identifying spatial biomarker signatures of predictive value. This study also further highlights the importance of robust end-to-end workflows to deliver optimal staining, imaging, and analysis to facilitate spatial phenotyping or analysis and interpretation in pathologically complex human tissue samples for the development of spatial signatures.

A Comprehensive Framework for Spatial Applications

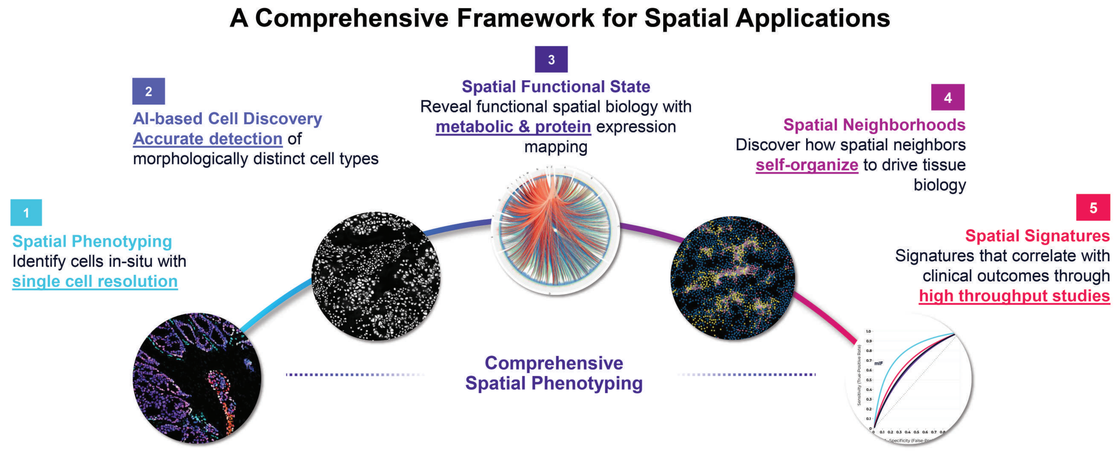

OracleBio AKOYA BIOSCIENCES®